Influence of ENSO on North American subseasonal surface air temperature variability

Patrick Martineau[1], Hisashi Nakamura[1,2], and Yu Kosaka[1]

[1]Research Center for Advanced Science and Technology, The University of Tokyo, Tokyo, Japan
[2]Japan Agency for Marine-Earth Science and Technology, Yokohama, Japan

Correspondence to: Patrick Martineau (pmartineau@atmos.rcast.u-tokyo.ac.jp)

Abstract. The wintertime influence of El Niño-Southern Oscillation (ENSO) on subseasonal variability is revisited by identifying the dominant mode of covariability between 10-60 day band-pass-filtered surface air temperature (SAT) variability over the North American continent and winter-mean sea surface temperature (SST) over the North Pacific sector. We find, in agreement with previous studies, that La Niña conditions tend to enhance the subseasonal SAT variability over western North America. This modulation of subseasonal variability is achieved through interactions between subseasonal eddies and La Niña-related changes in the winter-mean circulation. Specifically, eastward-propagating quasi-stationary eddies over the North Pacific are more efficient in extracting energy from the mean flow through the baroclinic conversion of energy over the North Pacific sector during La Niña. Changes in the vertical structure of these wave anomalies are crucial to enhance the efficiency of energy conversion via amplified downgradient heat fluxes that energize subseasonal eddy thermal anomalies. The combination of increased subseasonal SAT variability and the cold winter-mean response to La Niña both contribute to enhancing the likelihood of cold extremes over western North America.

1 Introduction

El Niño-Southern Oscillation (ENSO), the leading mode of sea surface temperature (SST) variability over the tropical Pacific sector, has far-reaching impacts on the atmospheric circulation in the Northern Hemisphere through the generation and propagation of a stationary Rossby wave train to the extratropics (Trenberth et al., 1998). This wave train originates in the western subtropical North Pacific, propagates initially northward, and refracts towards North America. It projects strongly on the dominant modes of atmospheric variability over the North Pacific Sector (Alexander et al., 2002; Horel and Wallace, 1981), including the Pacific North American (PNA) pattern (Wallace and Gutzler, 1981), under the feedback forcing from the modulated stormtrack activity (Lau, 1997). The atmospheric response to the warm phase of ENSO (El Niño) is characterized by a strengthening of the North Pacific jet stream that also stretches further eastward, and vice versa for the cool phase (La Niña).

In addition to its effect on the extratropical winter-mean atmospheric circulation, ENSO also influences intraseasonal variability. Nakamura (1996) identified a mode of year-to-year covariability between the winter-mean tropospheric

30   circulation and subseasonal variability over the North Pacific sector. This mode is characterized by extratropical winter-mean circulation anomalies that strongly resemble the atmospheric response to ENSO and the PNA pattern. More specifically, winter-mean anticyclonic anomalies that are associated with the weakened surface Aleutian Low and with the negative phase of the PNA tend to be accompanied by an increase of subseasonal variability over the North Pacific. The associated SST anomalies are characterized by warm anomalies in the central North Pacific, indicative of a possible

35   connection with La Niña. Similarly, Renwick and Wallace (1996) noted an increase of subseasonal variability over the North Pacific in La Niña winters. Since then, many studies have confirmed ENSO's modulations of subseasonal variability (Chen and Dool, 1999; Chen and van den Dool, 1997; Compo et al., 2001; Tam and Lau, 2005). This influence of ENSO on subseasonal variability not only affects the mid-tropospheric flow as shown in many of these studies but also has a clear impact on surface air temperature (SAT), potentially modulating the occurrence of weather extremes. In fact, Smith and

40   Sardeshmukh (2000) have shown that the intraseasonal temperature variance is enhanced over the North American West Coast during La Niña conditions.

In agreement with ENSO's modulation of subseasonal variability, blocking events, which are prominent and persistent atmospheric circulation anomalies that exert an important influence on SAT variability (Buehler et al., 2011; Martineau et al., 2017; Pfahl and Wernli, 2012; Rex, 1950), were also shown to occur preferentially for a specific phase of ENSO. Several

45   studies have noted an enhancement of blocking activity during La Niña (Barriopedro and Calvo, 2014; Chen and van den Dool, 1997; Renwick and Wallace, 1996), while others have rather noted a shift in the preferred location of blocking (Mullen, 1989) or even a decrease in blocking occurrence (Gollan and Greatbatch, 2017; Hinton et al., 2009) during La Niña. These discrepancies likely stem from conceptual differences in the definition of blocking events, which are sometimes defined as a reversal of the zonal flow in the mid-latitudes and other times as prominent anticyclonic anomalies.

50   Several mechanisms have been proposed to explain ENSO's influence on extratropical subseasonal variability. Tam and Lau (2005) suggested that changes in the tropical source of quasi-stationary Rossby eddies, resulting from ENSO's influence on MJO activity, and changes in the propagation of these wave trains under the modulated refractive properties of the mid-latitude westerlies by ENSO were among the plausible causes. Changes in barotropic energy conversion, i.e. the direct transfer of kinetic energy between the climatological jet stream and subseasonal eddies, forced by ENSO variability, and

55   changes in the feedback forcing by high-frequency eddies due to shifts in the preferred location of the storm track were also proposed as possible mechanisms (Chen and Dool, 1999; Chen and van den Dool, 1997). High-frequency eddy feedback and interactions between low-frequency variability and the mean flow were also shown to contribute strongly to the enhancement of subseasonal variability during the negative phase of the PNA (Lin and Derome, 1997) and thus may also be effective during La Niña winters.

60   Previous studies often assumed that subseasonal variability is predominantly equivalent barotropic, i.e., with structures that have slight or no vertical tilts, and thus the dynamical processes linked to the vertical dependence of their structure remain poorly understood. Tam and Lau (2005) nevertheless noted a vertical dependence of the structure of the quasi-stationary waves associated with subseasonal variability over the North Pacific. They have discussed the possibility, without evaluating

it, however, that baroclinic processes may play a role. Recently, Sung et al. (2019) found that the recent decadal shift of the Tropical Pacific into La Niña-like condition have modified baroclinic energy conversion into the North Pacific Oscillation (NPO; (Barnston and Livezey, 1987; Linkin and Nigam, 2008; Wallace and Gutzler, 1981), leading to enhanced temperature extremes over North America. It is thus plausible that ENSO's influence on subseasonal variability may result, at least in part, from the modulated baroclinicity of the seasonal-mean circulation in the extratropics and the vertical structure of eddies. This hypothesis is reasonable since subseasonal variability does exhibit vertically-tilting structures (Blackmon et al., 1979; Cai et al., 2007; Dole, 1986; Taguchi and Asai, 1987) which play an important role in energizing these eddies (Cai et al., 2007; Sheng and Derome, 1991; Tanaka et al., 2016).

The key goal of this work is thus to assess the role of baroclinic processes in ENSO's modulations of subseasonal variability over the North Pacific sector. As a first step, we identify the dominant mode of covariability between North-Pacific SST anomalies and subseasonal SAT variability affecting the eastern Pacific sector and North American continent through a singular value decomposition analysis. By focusing on surface variability instead of mid-tropospheric variability, this study aims to better understand the dynamical processes that regulate persistent SAT anomalies that have large socio-economic impacts. Without surprise, ENSO-like SST variability emerges from this analysis as the dominant influence on North American subseasonal SAT variability. In agreement with Smith and Sardeshmukh (2000), La Niña conditions tend to enhance the variability over Western North America.

As a second step, we evaluate how changes in the extratropical winter-mean circulation forced by ENSO modulate subseasonal eddy energy. The roles of baroclinic and barotropic energy conversions from the winter-mean flow to subseasonal eddies are assessed. In addition, we also assess the roles of high-frequency eddy feedback and diabatic processes in the energetics. From this analysis, baroclinic energy conversion, which is tied to the vertically-tilting structure of subseasonal circulation anomalies, stands out as the primary source of energy by which ENSO modulates subseasonal variability.

Concerning ENSO's influence on the frequency of warm and cold temperature extremes, we find that the impacts of ENSO on both winter-mean SAT and subseasonal SAT variability contribute to the enhanced likelihood of cold extremes over North America during La Niña.

2 Methodology

2.1 Data

This study uses reanalysis data from the Japan Meteorological Agency 55-year Reanalysis (JRA-55, Kobayashi et al. 2015) from 1958 to 2016. Variables analysed include the three-dimensional wind field (u, v, ω), temperature (T), geopotential height (Z), parameterized diabatic heating (Q) and temperature 2 meters above the surface (SAT). SST is obtained from the HadISST dataset (Rayner et al., 2003).

2.2 Singular value decomposition analysis

Singular value decomposition (SVD) analysis (Bjornsson and Venegas, 1997; Bretherton et al., 1992) is used to identify the dominant mode of covariability between winter-mean (December-January-February) SST over the Pacific sector (5°S-60°N, 140°E-80°W) and subseasonal SAT variability (SSV; local standard deviation of 10-60 day bandpass-filtered SAT) over the Eastern North Pacific and North-American sectors (10°N-60°N, 170°W-60°W). The sectors used for the two variables are illustrated in Fig. 1 with dashed rectangles. Results are not sensitive to small variations in these sectors. After obtaining the SST and SSV patterns from the SVD analysis, time series expressing their time evolution (SVD1$_{SST}$ and SVD1$_{SSV}$) are obtained by projecting the original SST and SSV anomaly fields onto these patterns. The SST and SSV patterns shown in this study are not the original patterns directly obtained from the SVD but rather heterogeneous regressions, i.e., SSV regressed onto SVD1$_{SST}$ and SST regressed onto SVD1$_{SSV}$. The heterogeneous patterns are similar to the original homogeneous patterns indicating strong coupling between the two fields. The statistical significance of the regressed heterogeneous patterns is assessed with a *t*-test for the correlation coefficient at the 95% confidence level.

2.3 ENSO indices

The SVD1$_{SST}$ time series is compared to classical ENSO indices to identify the index that is optimally related to North American SAT variability. The ENSO indices are obtained by averaging SST anomalies over various sectors followed by a normalization of each index. The sectors are [10°S-0°, 90°W-80°W] for Niño1+2, [5°S-5°N, 150°W-90°W] for Niño3, [5°S-5°N, 170°W-120°W] for Niño3.4, and [5°S-5°N, 160°E-150°W] for Niño4 (Bamston et al., 1997).

2.4 Energetics of subseasonal eddies

Atmospheric energetics (Lorenz, 1955; Oort, 1964) are used to assess how ENSO modulates the sources of energy sustaining circulation anomalies to produce subseasonal SAT variability. Energies and their conversion/generation terms are integrated vertically from the surface to 100 hPa for subseasonal variability that has been extracted by applying a 10-60 day bandpass filter (denoted with primes in the following equations). The basic state, denoted with overbars, is defined as the winter-mean (DJF) fields for individual years, which include fluctuations related to ENSO variability.

The eddy available potential energy (EAPE), is defined as

$$\text{EAPE} = \gamma^{-1} \frac{T'^2}{2}, \tag{1}$$

where γ is a stability parameter defined as

$$\gamma = \frac{p}{R}\left(\frac{R\hat{\bar{T}}}{C_p p} - \frac{\partial \hat{\bar{T}}}{\partial p}\right). \tag{2}$$

Here R is the gas constant for dry air (287 J K^{-1} kg^{-1}) and Cp is the specific heat at constant pressure (1004 J K^{-1} kg^{-1}). The stability parameter is here based on temperature averaged over the Northern Hemisphere (denoted by the hat operator). The

EAPE is proportional to temperature variance when averaged over a season and receives a strong contribution from the

125   lower troposphere where subseasonal temperature anomalies are strongest (not shown).

Several sources of EAPE are considered. The first is baroclinic energy conversion (CP):

$$\text{CP} = -\gamma^{-1}\left(u'T'\frac{\partial \bar{T}}{\partial x} + v'T'\frac{\partial \bar{T}}{\partial y}\right). \tag{3}$$

It describes how available potential energy is transferred from the winter-mean flow to subseasonal eddies, which is

achieved through downgradient eddy heat fluxes. We also consider feedback forcing on EAPE by high-frequency eddies

130   (double primes; Tanaka et al., 2016):

$$\text{CP}_{\text{HF}} = -\gamma^{-1}T'\left(\frac{\partial (u''T'')'}{\partial x} + \frac{\partial (v''T'')'}{\partial y}\right). \tag{4}$$

CP_{HF} describes how high-frequency eddy heat fluxes act to reinforce or dampen subseasonal temperature anomalies.

Diabatic processes can also play a role in the maintenance or dissipation of EAPE. It is evaluated here with

$$\text{CQ} = \gamma^{-1}\frac{Q'T'}{c_p}, \tag{5}$$

135   where Q is the heating rate. Diabatic processes and parameterized vertical heat diffusion, which are provided by JRA-55, are

all included in Q.

We also investigate ENSO's modulation of eddy kinetic energy (EKE), defined as

$$\text{EKE} = \frac{u'^2 + v'^2}{2}, \tag{6}$$

where u' and v' are wind anomalies associated with subseasonal eddies. The sources of EKE considered here include

140   barotropic energy conversion (CK) from the seasonal-mean flow to subseasonal eddies (Oort, 1964; Simmons et al., 1983)

$$\text{CK} = \frac{v'^2 - u'^2}{2}\left(\frac{\partial \bar{u}}{\partial x} - \frac{\partial \bar{v}}{\partial y}\right) - u'v'\left(\frac{\partial \bar{u}}{\partial y} + \frac{\partial \bar{v}}{\partial x}\right), \tag{7}$$

the feedback forcing from high-frequency eddies (CK_{HF}; Tanaka et al. (2016)) defined as

$$\text{CK}_{\text{HF}} = -u'\left(\frac{\partial (u''u'')'}{\partial x} + \frac{\partial (u''v'')'}{\partial y}\right) - v'\left(\frac{\partial (u''v'')'}{\partial x} + \frac{\partial (v''v'')'}{\partial y}\right), \tag{8}$$

and transfers of energy between EAPE and EKE

145    $$\text{CPK} = -\text{CKP} = -\frac{R\omega'T'}{p}, \tag{9}$$

which is achieved through vertical motion. Here a positive CPK denotes a transfer from EAPE to EKE and *vice-versa*.

The spatial redistribution of energy by mean flow related fluxes of energy ($-\nabla \cdot \bar{u}(EAPE + EKE)$) and pressure work ($-\nabla \cdot$

$(u'\Phi')$) are not assessed in this work since they have no net contribution to the modulation of subseasonal eddy energy after

integrated over a large domain.

150   We here evaluate the efficiency of energy conversion by normalizing the conversion terms by the total eddy energy (EAPE +

EKE) for each winter. For instance, the efficiency of CP may be evaluated as CP^{eff}, which is defined as

$$\text{CP}^{\text{eff}} = \frac{\langle \text{CP} \rangle}{\langle EAPE + EKE \rangle}, \tag{10}$$

where the angle brackets denote an average over the months of DJF, a vertical integral from the surface to 100 hPa and integration over the North Pacific (10°-87.5°N, 120°E-55°W).

3 Results

3.1 ENSO's influence on North American surface temperature variability

The dominant mode of covariability (SVD1) between SSV and SST explains about 56% of the total squared covariance between the two fields (Fig. 1). It is characterized by a significant increase of SSV (up to ~10% of the climatology) over the western U.S., Canada, Alaska, and Eastern Siberia, in association with cold SST anomalies over the Eastern Equatorial Pacific and warm anomalies over the Western Equatorial Pacific. These significant SST anomalies are strongly reminiscent of the cold phase of ENSO, La Niña. Indeed, the time series representing the temporal variability of this pattern (SVD1$_{SST}$, Fig. 1c) is strongly anticorrelated to all the four Niño indices (Table 1). SVD1$_{SST}$ is most strongly anticorrelated to the Niño 3 and Niño 3.4 indices, indicating a dominant link between Eastern Equatorial Pacific variability and SSV over North America. The anti-correlations between SVD1$_{SSV}$ and two other Niño indices are also strong and statistically significant. Meanwhile, the correlation between SVD1$_{SST}$ and SVD1$_{SSV}$ is significant but rather modest, which suggests that factors other than ENSO, such as internal atmospheric variability or other teleconnections, may also affect subseasonal SAT variability in a similar manner. Such a possibility is briefly explored later.

The regression map of winter-mean 500-hPa Z (Z500) onto the SVD1$_{SSV}$ index (Fig. 1b) resembles La Niña's impact on the extratropical atmospheric circulation that features the negative phase of the PNA. Specifically, cyclonic anomalies are found over the Western subtropical Pacific and Canada and anticyclonic anomalies are over the midlatitude North Pacific north of 40°N. These anomalies constitute a Rossby wave train refracting around the Eastern North Pacific, as suggested by the wave-activity flux (Takaya and Nakamura, 2001). This anomaly pattern represents the weakened and more diffluent North Pacific jet (not shown).

3.2 Processes through which ENSO affects subseasonal eddy activity

In this section, we evaluate ENSO's influence on subseasonal eddy activity by assessing ENSO's modulation of various sources/sinks of eddy energy. For this analysis, all components of the winter-mean energy budget for subseasonal eddies described in Sect. 2.4 are regressed onto SVD1$_{SST}$. As a reminder, this index is strongly anticorrelated to the Niño 3.4 index. A positive SVD1$_{SST}$ index is, therefore, representative of ENSO's cold phase (La Niña), and all the regression patterns show the linear response to ENSO featuring its cold phase. Note that we have also carried out a composite analysis for El Niño and La Niña winters separately and found salient features to be mostly linear.

Figures 2a-b show anomalies of EAPE and EKE corresponding to a unit standard deviation of the SVD1$_{SST}$ index. Both EAPE and EKE tend to overall increase during La Niña conditions, the former of which is consistent with the enhanced SSV of SAT over the landmasses. Whereas the EAPE signal is mostly concentrated over landmasses north of the Pacific Ocean

and over North America, the EKE signal is particularly large over the subpolar North Pacific sector. Integrated over the
185   whole North Pacific (Fig. 3), the energy increase is roughly equipartitioned between EAPE and EKE, but slightly larger for
the latter.

Next, we examine the corresponding changes in the conversion of energy from the winter-mean flow to subseasonal eddies
through the baroclinic (CP) and barotropic (CK) conversions. A large increase in CP is observed over the subpolar North
Pacific with its maximum over the Gulf of Alaska, which contributes to an increase of CP^{eff} over the entire North Pacific
190   (Fig. 3). Like CP, CK also tends to increase over the North Pacific (Fig. 2d), but overall, the contribution of CK is weaker
than that of CP (Fig. 3).

As per their definition, CP and CK depend on both the winter-mean flow configuration and eddy properties. To assess their
relative importance, we compute composite differences between years when the normalized $SVD1_{SST}$ is above 0.5 or below
–0.5. The composite differences in which both the eddy properties and basic-state properties are allowed to vary from year to
195   year (Figs. 4e-f) are contrasted to the corresponding composites in which the basic-state properties (Figs. 4a-b) or eddy
properties (Figs. 4c-d) are set to their climatologies from 1979 to 2015. The comparison reveals that year-to-year changes in
eddy properties are essential to explain the enhanced CP over the Pacific sector (comparing Fig. 4a to Fig. 4e). Over the
sectors of enhanced CP, we find evidence of a stronger positive correlation between v' and T' (Fig. 5) throughout the depth
of the troposphere, which indicates that the structure of subseasonal eddies is more adequate to extract energy from the
200   meridional thermal gradient of the background state for their baroclinic growth. We also find that the climatologically
positive and negative correlations between u' and T' are enhanced over Alaska and the Okhotsk Sea, respectively, which also
contribute to the increased CP. Concerning CK, the enhanced conversion over Alaska results from changes in eddy
properties, while the changes over the Western North Pacific appear to result from a combination of changes in both eddy
and winter-mean flow properties (Fig. 4 right).

205   The contributions of CP and CK are found to be much larger than the feedback forcing by high-frequency transients (CP_{HF}
and CK_{HF}), which are weak and contribute minimally to changes in the energetics (Figs. 2e-f and 3). Similarly, diabatic
feedback (CQ) has a negligible contribution.

Finally, we also investigate the transfer (CPK) between EAPE and EKE. We find that CPK is enhanced over a broad domain
stretching from the western subtropical North Pacific to Alaska (Fig. 2h). This sector is collocated with the region of
210   enhanced CP (Fig. 2c), which indicates that an important portion of the gains in EAPE through CP is transferred to EKE in-
situ. This transfer is small compared to CP, but about half of CK and thus relevant to the observed increase in EKE. Changes
in the correlation between ω' and T' are overall not well organized (Fig. 5) which suggests that changes in CPK are mostly
due to changes in the magnitudes of the eddy terms rather than to eddies' structures.

3.3 Changes in propagation and structure of subseasonal eddies

215 In this section, we assess ENSO's influence on the propagation of wave activity and the structure of subseasonal eddies. Subseasonal eddy propagation is first assessed by using the wave activity flux for stationary Rossby waves (Takaya and Nakamura, 1997, 2001) computed from 10-60 day band-pass filtered Z500. The flux, which is climatologically eastward (not shown), tends to be enhanced during La Niña winters (Fig. 6). The enhanced eastward flux is observed over the subpolar North Pacific, where CP is enhanced, and over western North America, where SSV also increases noticeably. The eastward

220 wave-activity flux is also enhanced just east of the region of enhanced CK over the subtropical North Pacific.

Next, we evaluate through lag-regression analysis the typical structure of the quasi-stationary eddies that are associated with subseasonal SAT variability over western North America (Fig. 7). The analysis is carried out with reference SAT time series over Alaska and Colorado. These time series are normalized so that the regressed patterns represent circulation anomalies associated with typical SAT variability. The instantaneous regression map corresponding to Alaska SAT variability shows a

225 clear wave train propagating eastward (Fig. 7e). The wave train is mostly stationary with little phase propagation from lag –3 (day) to lag 0 (Figs. 7c,e). At all lags, positive correlations are observed over the subtropical North Pacific, suggesting a potential subtropical origin to this wave train. Precursors are also observed over Russia at lag –6 (Fig. 7a) as well as lags –9 and –12 (not shown), indicating that this wave train may also originate from the extratropics. The same instantaneous regression performed for a reference SAT index over Colorado also reveals an eastward-propagating wave train (Fig. 7f).

230 Through the lag regression analysis, the origin of this wave train can be traced back in part to the subpolar North Pacific and the subtropical central Pacific (Figs. 7b,d). In this case, the phase of the wave train is seen to move slowly eastward.

Both quasi-stationary wave structures revealed by the regression analysis propagate through the North Pacific sector where CP and CK are enhanced. Significant differences in the amplitude of these wave trains are observed between the two phases of SVD1$_{\mathrm{SST}}$. Differences in the Z500 regression pattern tend to be positive where the Z500 anomalies are typically positive

235 and *vice-versa*, which indicates an overall intensification of the amplitude of the wave patterns during La Niña conditions. It is consistent with the enhanced eddy energy and wave activity fluxes discussed previously.

To understand better how quasi-stationary eddies more efficiently extract energy from the winter-mean flow through heat fluxes during La Niña, we also analyse through one-point regressions the vertical structure of these eddies (Fig. 8). Their structure is evaluated over the North Pacific where the enhanced correlation between v' and T' (Fig. 5) hints to important

240 zonal structural changes. Indeed, the westward tilt of the geopotential height structure is enhanced when SVD1$_{\mathrm{SST}} > 1$, which is consistent with the enhanced v'-T' correlation. Whereas the westward tilt is found throughout the depth of the troposphere when SVD1$_{\mathrm{SST}} > 1$, it is weaker and limited to the lower troposphere when SVD1$_{\mathrm{SST}} < -1$. Also, geopotential height anomalies are out of phase with temperature anomalies at all levels when SVD1$_{\mathrm{SST}} > 1$, whereas they are out of phase only below 700 hPa when SVD1$_{\mathrm{SST}} < -1$. These changes in the vertical structure of subseasonal eddies, manifested also as the

245 enhanced positive v'-T' correlation (Fig. 5), allow for a more efficient downgradient heat transport during La Niña

(SVD1$_{SST}$ >1), thus leading to a more efficient extraction of energy from the winter-mean flow through baroclinic conversion (Fig. 3).

3.4 Impact on extreme temperature events

The impact of SVD1$_{SST}$/ENSO variability on the occurrence of persistent weather extremes is now investigated. Cold (warm)
250   extreme days are defined as the days when 10-day lowpass-filtered SAT anomaly falls below (rises above) the 5th (95th) percentiles over the 58 winters. Their frequency, calculated as the percentage of winter days, is then regressed onto the SVD1$_{SST}$ time series. The spatial patterns of changes in the frequency of weather extremes (Figs. 9a-b) are similar to the winter-mean SAT response (Fig. 9c) with an enhanced frequency of cold extremes over the regions that are colder than normal and *vice-versa*. Generally, the corresponding relationship holds also between warm extremes and winter-mean SAT.
255   This indicates that the winter-mean response to ENSO variability plays a major role in setting the frequency of extremes, through shifts in the probability distributions of temperature.

However, an important asymmetry is observed in the response of warm and cold extremes over western and southern North America (Figs. 9a-b). In Alaska and western Canada, colder winter-mean SAT under the La Niña conditions accompany an increase in the frequency of cold extremes, while the corresponding changes in the frequency of warm extremes are rather
260   small and insignificant over land. Likewise, in the southern U.S., the anomalous winter-mean warmth increases warm extremes but the frequency changes of cold extremes are small. These asymmetries arise from the enhanced subseasonal variability (Fig. 9d), which significantly widens the probability distribution of SAT over these sectors. Changes in skewness also contribute to altering the frequency of warm and cold extremes over some sectors, but their contribution is overall spatially less organized and also statistically insignificant (not shown).

265   3.5 Modulation of subseasonal SAT variability unrelated to ENSO

As mentioned earlier, SVD1$_{SSV}$ is moderately correlated to SVD1$_{SST}$ and Niño indices (Table 1), which suggests that a substantial fraction of year-to-year variations in SSV over the North American West Coast may arise from internal atmospheric variability. The processes responsible for this variability are briefly assessed. The component of SVD1$_{SSV}$ that is uncorrelated with SVD1$_{SST}$ (SVD1R$_{SSV}$) is first identified as the residual of the linear regression between the two indices. By
270   regressing SSV onto the index (Fig. 10a), we find an amplification of SSV whose spatial structure is similar to the one previously identified (Fig. 1a) and whose intensity is notably augmented over North America (up to ~15% of the climatology). The correlations of SVD1R$_{SSV}$ with the ENSO indices are weak overall and insignificant except for the Niño 4 index (Table 2). Consistently, the corresponding grid-by-grid correlation is significant only in the central Equatorial Pacific (Fig. 10b). Stronger SST anomalies are however found in the midlatitude North Pacific with a pattern somewhat reminiscent
275   of the North Pacific Gyre Oscillation (NPGO) (Di Lorenzo et al., 2008). While the winter-mean circulation pattern associated with SVD1R$_{SSV}$ (Fig. 10b) shares some similarities with the negative phase of the PNA, it is also similar to the negative phase of the NPO. In fact, Di Lorenzo et al. (2008) indicate that the NPGO is driven by wind stress curl anomalies

associated with the NPO. We argue that SVD1R$_{SSV}$-related variability is related to the internal variability of the eddy-driven jet over the North Pacific. The feedback of NPGO-like SST anomalies onto the atmospheric anomalies in Fig.10b needs to

280 be addressed in future studies. Like SVD1, SVD1R$_{SSV}$ enhances the efficiency of the baroclinic conversion of energy from the winter-mean flow over the North Pacific and the propagation of quasi-stationary waves towards North America (not shown), which acts to enhance SAT variability over the continent.

4 Summary

By identifying the dominant mode of interannual covariability between winter-mean SST and subseasonal SAT variability,
285 this study confirms the prominent role of ENSO in modulating the SAT variability over North America. El Niño and La Niña tend to enhance and reduce SAT variability, respectively (Smith and Sardeshmukh, 2000). Among the classical ENSO indices, the Niño 3 and Niño 3.4 indices are most closely associated with the mode of variability identified in this work.

Energetics of subseasonal atmospheric eddies reveals that La Niña is not only accompanied by an augmentation of EKE (Chen and Dool, 1999) but also by an increase of EAPE over the North Pacific sector, as consistent with the rise of
290 subseasonal SAT variability. In fact, the ENSO's modulation of baroclinic energy conversion is found more important than the barotropic processes emphasized in previous studies (Chen and van den Dool, 1997; Tam and Lau, 2005). The baroclinic energy conversion is achieved through eddy heat fluxes that are downgradient of the temperature climatology. Alternatively, this conversion can be interpreted as the anomalous thermal advection by subseasonal eddies acting on the climatological temperature gradient in such a way that it reinforces eddy temperature anomalies. In contrast to the baroclinic energy
295 conversion, the feedback of high-frequency eddies, which was suggested as an important process (Chen and Dool, 1999; Chen and van den Dool, 1997), is much smaller. It is explained by the fact that previous studies have only assessed the budget of kinetic energy in the upper troposphere, which overemphasizes the feedback of high-frequency eddies on the kinetic energy (Lau and Nath, 1991) and overlooks the cancellation between high-frequency eddy feedbacks onto the eddy available potential energy and eddy kinetic energy (Tanaka et al., 2016).
300 Although lag-regression maps suggest that the subseasonal eddies affecting SAT over North America originate in part from the Tropics, the modulation of subseasonal eddy energetics by ENSO is dominated by baroclinic energy conversions in the mid to high latitudes. This suggests that ENSO's influence is not a simple manifestation of modulated tropical sources of subseasonal variability, as suggested by Tam and Lau (2005). This conclusion is also supported by the absence of significant changes in EAPE or EKE in the Tropics and the fact that the modulation of energy sources by diabatic processes is
305 comparatively very small. It is more likely that subseasonal wave trains forced by normal levels of tropical convective activity can extract more energy from the winter-mean westerlies as they propagate through the mid and high latitudes under La Niña conditions.

We have further revealed that changes in the properties of subseasonal eddies are essential for the enhancement of baroclinic energy conversion during La Niña. In comparison, ENSO-related changes in background flow properties have a rather

310   modest direct impact on the energetics. The background flow properties, however, may have an indirect impact through their influence on the propagation and structure of subseasonal eddies. Over the midlatitude North Pacific eddy velocity and temperature anomalies are overall better correlated during La Niña, which translates into larger downgradient eddy heat fluxes and consequently into more efficient baroclinic energy conversion. The enhanced correlation results from a more pronounced vertical tilt of eddies and the more out-of-phase relationship of the maxima of geopotential height and
315   temperature throughout the depth of the troposphere.

 Our analysis thus suggests that, during La Niña, the growth of subseasonal eddies is enhanced over the North Pacific as they propagate towards North America. Once they reach the North American coast, these eddies have strong signatures in lower-tropospheric temperatures, due to the reduced near-surface damping of temperature anomalies over land in comparison to over the ocean, thereby enhancing SAT variability. This enhanced variability, combined with cold winter-mean temperature
320   anomalies during La Niña, contributes to enhancing the likelihood of persistent cold extremes, especially over western North America. Our analysis is thus in agreement with the recent finding by Sung et al. (2019) that interdecadal La Niña-like conditions can enhance temperature extremes over North America through modulated baroclinic energy conversion of NPO anomalies, and we have confirmed that similar processes are operative also with interannual ENSO variability.

In addition to ENSO's influence, an important fraction of subseasonal SAT variability over North America appears related to
325   interannual PNA-like or NPO-like atmospheric variability that is uncorrelated with ENSO. Our ability to forecast subseasonal variance over North America may thus depend on the forecast skill of these other atmospheric teleconnections and thus on whether they are externally forced or purely internally generated.

Code availability

The codes used in this paper can be obtained from the authors upon request.

330   **Data availability**

JRA-55 (Japan Meteorological Agency, 2013) was obtained from the NCAR/UCAR Research Data Archive (RDA). The HadISST dataset was obtained from the Met Office Hadley Centre.

Author contribution

All authors designed the analysis and edited the paper. PM performed the calculations, plotted the results, and drafted the
335   original paper.

Competing interests

The authors declare that they have no conflict of interest.

Acknowledgements

This study is supported in part by the Japanese Ministry of Education, Culture, Sports, Science and Technology (MEXT)
340 through the Arctic Challenge for Sustainability (ArCS) Program and the Integrated Research Program for Advancing
Climate Models (JPMXD0717935457), by the Japan Science and Technology Agency through Belmont Forum CRA
"InterDec", by the Japanese Ministry of Environment through Environment Research and Technology Development Fund 2-
1904, and by the Japan Society for the Promotion of Science (JSPS) through Grants-in-Aid for Scientific Research
JP16H01844, JP18H01278, JP18H01281, JP19H05702 and JP19H05703 (on Innovative Areas 6102). PM is partly
345 supported by Grant-in-Aid for JSPS Research Fellow.

References

Alexander, M. A., Bladé, I., Newman, M., Lanzante, J. R., Lau, N.-C. and Scott, J. D.: The Atmospheric Bridge: The
Influence of ENSO Teleconnections on Air–Sea Interaction over the Global Oceans, J. Clim., 15(16), 2205–2231,
doi:10.1175/1520-0442(2002)015<2205:TABTIO>2.0.CO;2, 2002.

350 Bamston, A. G., Chelliah, M. and Goldenberg, S. B.: Documentation of a highly ENSO-related sst region in the equatorial
pacific: Research note, Atmosphere-Ocean, 35(3), 367–383, doi:10.1080/07055900.1997.9649597, 1997.

Barnston, A. G. and Livezey, R. E.: Classification, Seasonality and Persistence of Low-Frequency Atmospheric Circulation
Patterns, Mon. Weather Rev., 115(6), 1083–1126, doi:10.1175/1520-0493(1987)115<1083:CSAPOL>2.0.CO;2, 1987.

Barriopedro, D. and Calvo, N.: On the Relationship between ENSO, Stratospheric Sudden Warmings, and Blocking, J.
355 Clim., 27(12), 4704–4720, doi:10.1175/JCLI-D-13-00770.1, 2014.

Bjornsson, H. and Venegas, S. A.: A Manual for EOF and SVD Analyses of Climatic Data, Department of Atmospheric and
Oceanic Sciences and Centre for Climate and Global Change Research: McGill University, Montreal, Quebec., 1997.

Blackmon, M. L., Madden, R. A., Wallace, J. M. and Gutzler, D. S.: Geographical Variations in the Vertical Structure of
Geopotential Height Fluctuations 1, J. Atmos. Sci., 36(12), 2450–2466, doi:10.1175/1520-
360 0469(1979)036<2450:GVITVS>2.0.CO;2, 1979.

Bretherton, C. S., Smith, C. and Wallace, J. M.: An Intercomparison of Methods for Finding Coupled Patterns in Climate
Data, J. Clim., 5(06), 541–560, doi:10.1175/1520-0442(1992)005<0541:AIOMFF>2.0.CO;2, 1992.

Buehler, T., Raible, C. C. and Stocker, T. F.: The relationship of winter season North Atlantic blocking frequencies to
extreme cold or dry spells in the ERA-40, Tellus, Ser. A Dyn. Meteorol. Oceanogr., 63(2), 212–222, doi:10.1111/j.1600-
365 0870.2010.00492.x, 2011.

Cai, M., Yang, S., Van Den Dool, H. M. and Kousky, V. E.: Dynamical implications of the orientation of atmospheric eddies: A local energetics perspective, Tellus, Ser. A Dyn. Meteorol. Oceanogr., 59(1), 127–140, doi:10.1111/j.1600-0870.2006.00213.x, 2007.

Chen, W. Y. and van den Dool, H. M.: Asymmetric Impact of Tropical SST Anomalies on Atmospheric Internal Variability over the North Pacific, J. Atmos. Sci., 54(6), 725–740, doi:10.1175/1520-0469(1997)054<0725:AIOTSA>2.0.CO;2, 1997.

Chen, W. Y. and Dool, H. M. Van Den: Significant change of extratropical natural variability and potential predictability associated with the El Niño/Southern Oscillation, Tellus A Dyn. Meteorol. Oceanogr., 51(5), 790–802, doi:10.3402/tellusa.v51i5.14493, 1999.

Compo, G. P., Sardeshmukh, P. D. and Penland, C.: Changes of Subseasonal Variability Associated with El Niño, J. Clim., 14(16), 3356–3374, doi:10.1175/1520-0442(2001)014<3356:COSVAW>2.0.CO;2, 2001.

Dole, R. M.: Persistent Anomalies of the Extratropical Northern Hemisphere Wintertime Circulation: Structure, Mon. Weather Rev., 114(1), 178–207, doi:10.1175/1520-0493(1986)114<0178:PAOTEN>2.0.CO;2, 1986.

Gollan, G. and Greatbatch, R. J.: The relationship between Northern Hemisphere winter blocking and tropical modes of variability, J. Clim., 30(22), 9321–9337, doi:10.1175/JCLI-D-16-0742.1, 2017.

Hinton, T. J., Hoskins, B. J. and Martin, G. M.: The influence of tropical sea surface temperatures and precipitation on north Pacific atmospheric blocking, Clim. Dyn., 33(4), 549–563, doi:10.1007/s00382-009-0542-7, 2009.

Horel, J. D. and Wallace, J. M.: Planetary-Scale Atmospheric Phenomena Associated with the Southern Oscillation, Mon. Wea. Rev., 109, 813–829, 1981.

Kobayashi, S., Ota, Y., Harada, Y., Ebita, A., Moriya, M., Onoda, H., Onogi, K., Kamahori, H., Kobayashi, C., Endo, H., Miyaoka, K. and Takahashi, K.: The JRA-55 Reanalysis: General Specifications and Basic Characteristics, J. Meteorol. Soc. Japan. Ser. II, 93(1), 5–48, doi:10.2151/jmsj.2015-001, 2015.

Lau, N.-C.: Interactions between Global SST Anomalies and the Midlatitude Atmospheric Circulation, Bull. Am. Meteorol. Soc., 78(1), 21–33, doi:10.1175/1520-0477(1997)078<0021:IBGSAA>2.0.CO;2, 1997.

Lau, N.-C. and Nath, M. J.: Variability of the Baroclinic and Barotropic Transient Eddy Forcing Associated with Monthly Changes in the Midlatitude Storm Tracks, J. Atmos. Sci., 48(24), 2589–2613, doi:10.1175/1520-0469(1991)048<2589:VOTBAB>2.0.CO;2, 1991.

Lin, H. and Derome, J.: On the modification of the high- and low-frequency eddies associated with the PNA anomaly: an observational study, Tellus A Dyn. Meteorol. Oceanogr., 49(1), 87–99, doi:10.3402/tellusa.v49i1.12213, 1997.

Linkin, M. E. and Nigam, S.: The North Pacific Oscillation-West Pacific teleconnection pattern: Mature-phase structure and winter impacts, J. Clim., 21(9), 1979–1997, doi:10.1175/2007JCLI2048.1, 2008.

Lorenz, E. N.: Available Potential Energy and the Maintenance of the General Circulation, Tellus, 7(2), 157–167, doi:10.3402/tellusa.v7i2.8796, 1955.

Di Lorenzo, E., Schneider, N., Cobb, K. M., Franks, P. J. S., Chhak, K., Miller, A. J., McWilliams, J. C., Bograd, S. J., Arango, H., Curchitser, E., Powell, T. M. and Rivière, P.: North Pacific Gyre Oscillation links ocean climate and ecosystem

400   change, Geophys. Res. Lett., 35(8), 2–7, doi:10.1029/2007GL032838, 2008.

Martineau, P., Chen, G. and Burrows, A. D.: Wave Events: Climatology, Trends, and Relationship to Northern Hemisphere Winter Blocking and Weather Extremes, J. Clim., 30(15), 5675–5697, doi:10.1175/JCLI-D-16-0692.1, 2017.

Mullen, S. L.: Model Experiments on the Impact of Pacific Sea Surface Temperature Anomalies on Blocking Frequency, J. Clim., 2(9), 997–1013, doi:10.1175/1520-0442(1989)002<0997:MEOTIO>2.0.CO;2, 1989.

405   Nakamura, H.: Year-to-Year and interdecadal variability in the activity of intraseasonal fluctuations in the Northern Hemisphere wintertime circulation, Theor. Appl. Climatol., 55(1–4), 19–32, doi:10.1007/BF00864700, 1996.

Oort, A. H.: On Estimates Of The Atmospheric Energy Cycle, Mon. Weather Rev., 92(11), 483–493, doi:10.1175/1520-0493(1964)092<0483:OEOTAE>2.3.CO;2, 1964.

Pfahl, S. and Wernli, H.: Quantifying the relevance of atmospheric blocking for co-located temperature extremes in the
410   Northern Hemisphere on (sub-)daily time scales, Geophys. Res. Lett., 39(12), 1–6, doi:10.1029/2012GL052261, 2012.

Rayner, N. A., Parker, D. E., Horton, E. B., Folland, C. K., Alexander, L. V., Rowell, and D. P., Kent, E. C. and Kaplan, A.: Global analyses of sea surface temperature, sea ice, and night marine air temperature since the late nineteenth century, J. Geophys. Res., 108(D14), 4407, doi:10.1029/2002JD002670, 2003.

Renwick, J. a. and Wallace, J. M.: Relationships between North Pacific Wintertime Blocking, El Niño, and the PNA Pattern,
415   Mon. Weather Rev., 124(9), 2071–2076, doi:10.1175/1520-0493(1996)124<2071:RBNPWB>2.0.CO;2, 1996.

Rex, D. F.: Blocking Action in the Middle Troposphere and its Effect upon Regional Climate. I. An Aerological Study of Blocking Action, Tellus, 2, 196–211, doi:10.1111/j.2153-3490.1950.tb00331.x, 1950.

Sheng, J. and Derome, J.: An observational study of the energy transfer between the seasonal mean flow and transient eddies, Tellus A, 43(2), 128–144, doi:10.1034/j.1600-0870.1991.t01-1-00004.x, 1991.

420   Simmons, a. J., Wallace, J. M. and Branstator, G. W.: Barotropic Wave Propagation and Instability, and Atmospheric Teleconnection Patterns, J. Atmos. Sci., 40(6), 1363–1392, doi:10.1175/1520-0469(1983)040<1363:BWPAIA>2.0.CO;2, 1983.

Smith, C. A. and Sardeshmukh, P. D.: The effect of ENSO on the intraseasonal variance of surface temperatures in winter, Int. J. Climatol., 20(13), 1543–1557, doi:10.1002/1097-0088(20001115)20:13<1543::AID-JOC579>3.0.CO;2-A, 2000.

425   Sung, M.-K., Jang, H.-Y., Kim, B.-M., Yeh, S.-W., Choi, Y.-S. and Yoo, C.: Tropical influence on the North Pacific Oscillation drives winter extremes in North America, Nat. Clim. Chang., 9(5), 413–418, doi:10.1038/s41558-019-0461-5, 2019.

Taguchi, S. and Asai, T.: Statistical Characteristics of Long-Lived Large-Scale Disturbances in the Northern Hemisphere 500hPa Height Fields, J. Meteorol. Soc. Japan. Ser. II, 65(2), 221–236, doi:10.2151/jmsj1965.65.2_221, 1987.

430   Takaya, K. and Nakamura, H.: A formulation of a wave-activity flux for stationary Rossby waves on a zonally varying basic flow, Geophys. Res. Lett., 24(23), 2985–2988, doi:10.1029/97GL03094, 1997.

Takaya, K. and Nakamura, H.: A Formulation of a Phase-Independent Wave-Activity Flux for Stationary and Migratory Quasigeostrophic Eddies on a Zonally Varying Basic Flow, J. Atmos. Sci., 58(6), 608–627, doi:10.1175/1520-

0469(2001)058<0608:AFOAPI>2.0.CO;2, 2001.

435 Tam, C. Y. and Lau, N. C.: The impact of ENSO on atmospheric intraseasonal variability as inferred from observations and GCM simulations, J. Clim., 18(12), 1902–1924, doi:10.1175/JCLI3399.1, 2005.

Tanaka, S., Nishii, K. and Nakamura, H.: Vertical structure and energetics of the Western Pacific teleconnection pattern, J. Clim., 29(18), 6597–6616, doi:10.1175/JCLI-D-15-0549.1, 2016.

Trenberth, K. E., Branstator, G. W., Karoly, D., Kumar, a, Lau, N. C. and Ropelewski, C.: Progress during TOGA in

440 understanding and modeling global teleconnections associated with tropical sea surface temperatures, J. Geophys. Res., 103(C7), 14291–14324, doi:10.1029/97jc01444, 1998.

Wallace, J. M. and Gutzler, D. S.: Teleconnections in the Geopotential Height Field during the Northern Hemisphere Winter, Mon. Weather Rev., 109(4), 784–812, doi:10.1175/1520-0493(1981)109<0784:TITGHF>2.0.CO;2, 1981.

445

Table 1: Pairwise correlation coefficients between SVD1$_{SSV}$, SVD1$_{SST}$, and the Niño indices (described in section 0). All correlations are significant at the 95% confidence level.

	SVD1$_{SST}$	Niño1+2	Niño3	Niño3.4	Niño4
SVD1$_{SSV}$	0.54	-0.35	-0.39	-0.37	-0.22
SVD1$_{SST}$		-0.79	-0.93	-0.90	-0.76

450

Table 2: Pairwise correlation coefficients between SVD1R$_{SSV}$ and the Niño indices (described in section 0). Correlations that are significant at the 95% confidence level are indicated in boldface.

	Niño1+2	Niño3	Niño3.4	Niño4
SVD1R$_{SSV}$	0.09	0.13	0.14	**0.23**
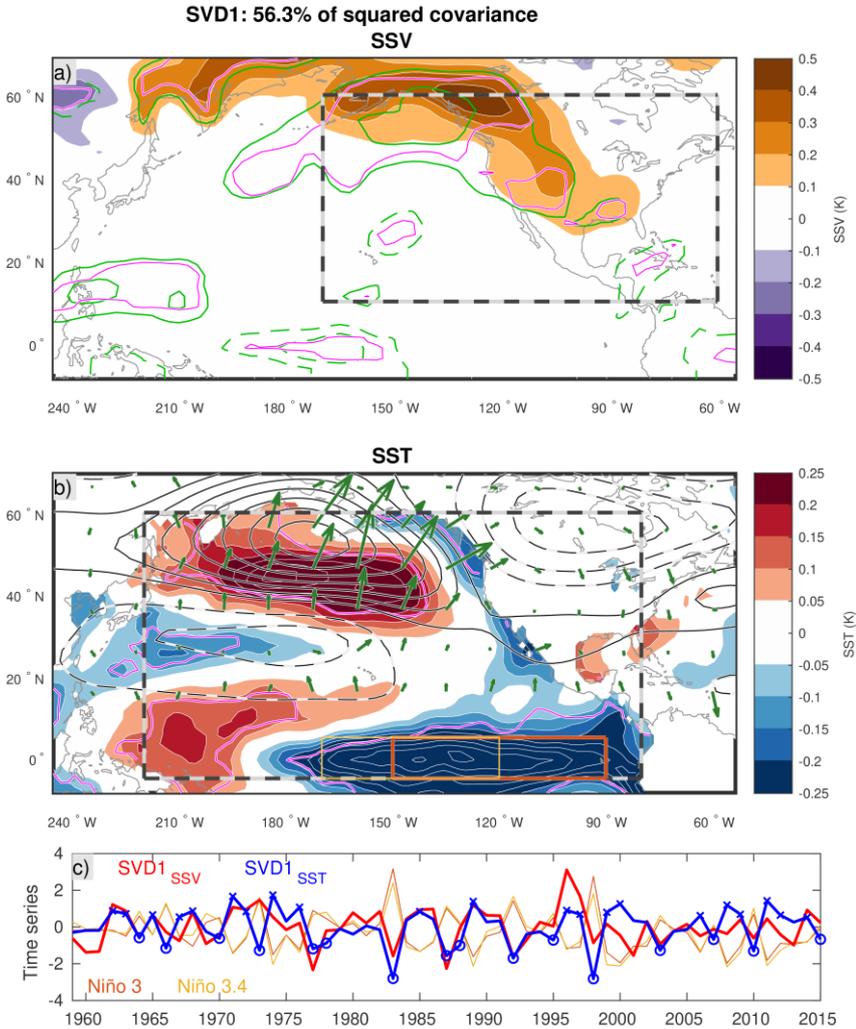
455

Figure 1: Wintertime anomaly patterns of a) SSV (subseasonal SAT variability) and b) winter-mean SST associated with the dominant mode of covariability (SVD1, corresponding to La Niña) between the two variables (color shadings; anomalies statistically significant at the 95% level are contoured in magenta). The sectors used for the SVD analysis are bounded by bold dashed lines. The green contours superimposed on a) indicate the fractional change of SSV relative to the climatology with 5%
460 **contour intervals (solid and dashed contours are used for positive and negative values, respectively; the 0 line is omitted). Z500 anomalies regressed onto SVD1$_{SST}$ are superimposed on b) with black contours (increment of 5 m, solid and dashed for positive and negative anomalies, respectively). The corresponding wave-activity fluxes** (Takaya and Nakamura, 2001) **are shown with green arrows. A distance of 1° corresponds to a flux of 0.125 m² s⁻². c) Anomaly time series of SSV (SVD1$_{SSV}$, red) and SST (SVD1$_{SST}$, blue) associated with SVD1. Two Niño indices are superimposed (domains used to compute these indices are illustrated over the**
465 **SST pattern in b).**
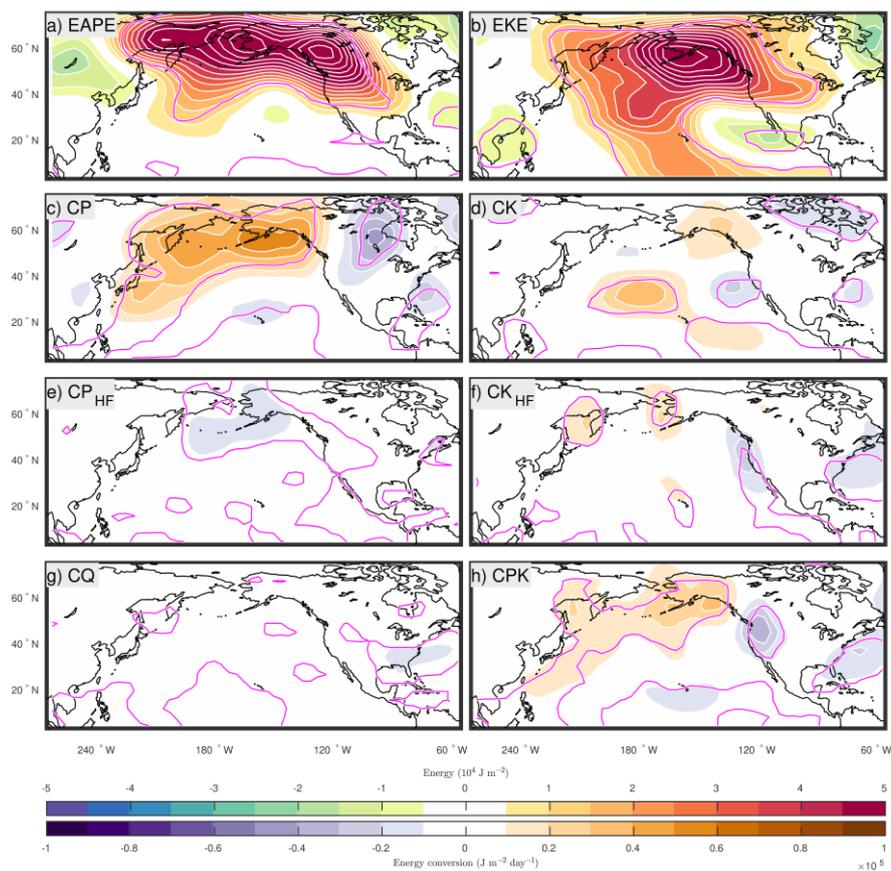
Figure 2: The a) EAPE and b) EKE of subseasonal eddies and energy sources/sinks (c-h) are regressed onto the SVD1$_{SST}$ index. Correlations that are statistically significant at the 95% confidence level are contoured in magenta.
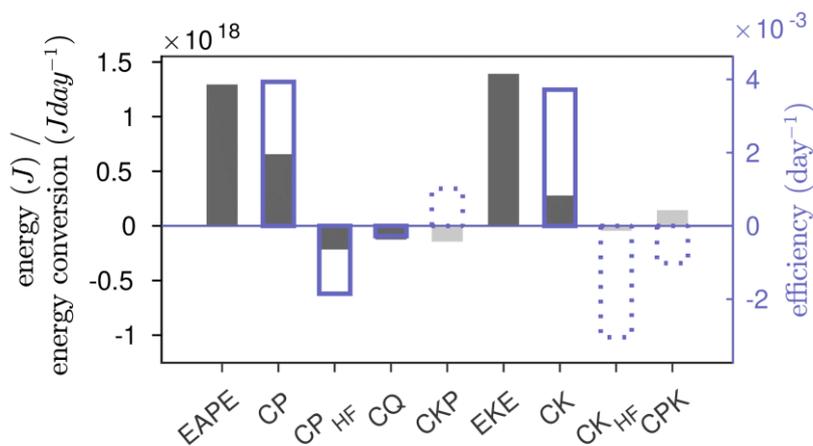
470   **Figure 3: The energetics of subseasonal eddies are integrated over the North Pacific (0°-87.5°N, 120°E-55°W) and regressed onto SVD1$_{SST}$. Raw changes in energy and sources/sinks are shown with solid bars. Significant values are shown with a darker shade of grey. Blue boxes indicate changes in the efficiency with significant changes indicated with solid borders.**
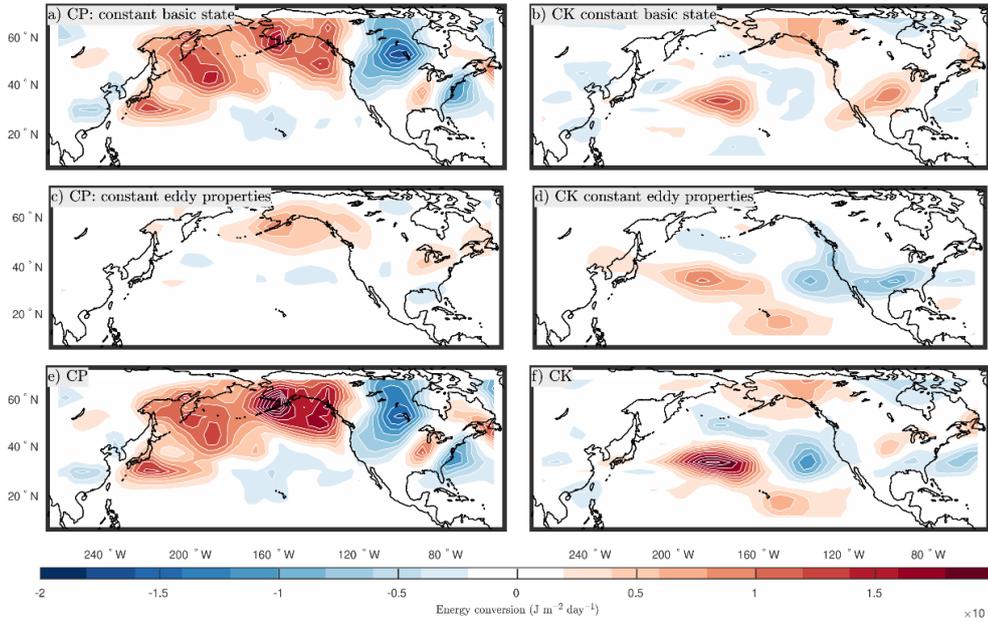
Figure 4: CP (left) and CK (right) composite differences between the positive and negative phases of SVD1 (representing La Niña) are calculated by keeping either the background flow properties (a,b) or eddy properties (c,d) constant every year. For reference, the composite difference when both eddy properties and the basic state can change from year to year is shown in e) and f).
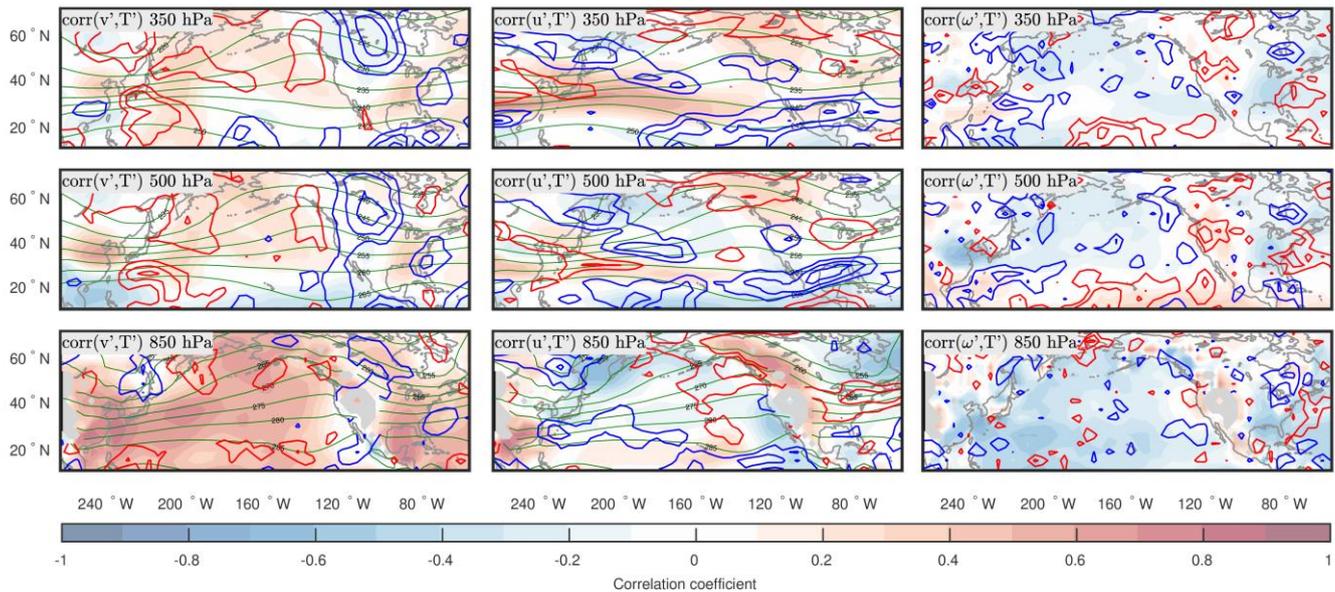
Figure 5: Composite differences of correlation coefficients between (left) v' and T', (centre) u' and T', and (right) ω' and T' between winters of SVD1$_{SST}$ > 0.5 and SVD1$_{SST}$ < −0.5. The composite difference is shown with blue and red contours with an interval of 0.1 for negative and positive values, respectively. The climatological correlation is shown with colour shadings. For reference, the temperature climatology is shown with green lines.
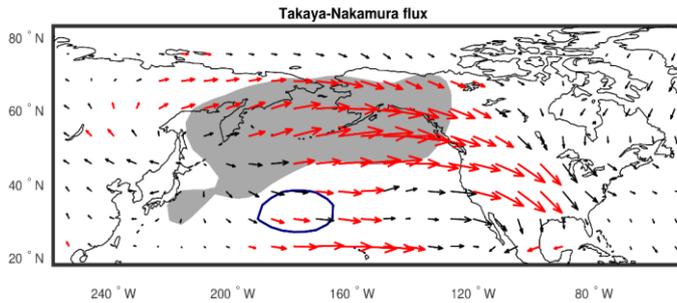
Figure 6: The wave-activity flux (Takaya and Nakamura, 2001) **of 10-60 day band-pass-filtered eddies regressed onto the SVD1$_{SST}$ time series. The anomalous flux whose meridional or vertical component is significant at the 95% level, assessed with a t-test on the correlation coefficients, are shown in red. A distance of 1° corresponds to a flux of 0.67 m²s⁻². Regions where CP and CK are larger than 3x10⁴ J m⁻² day⁻¹ are denoted with grey shading and a blue contour, respectively (see Figs. 2c-d).**
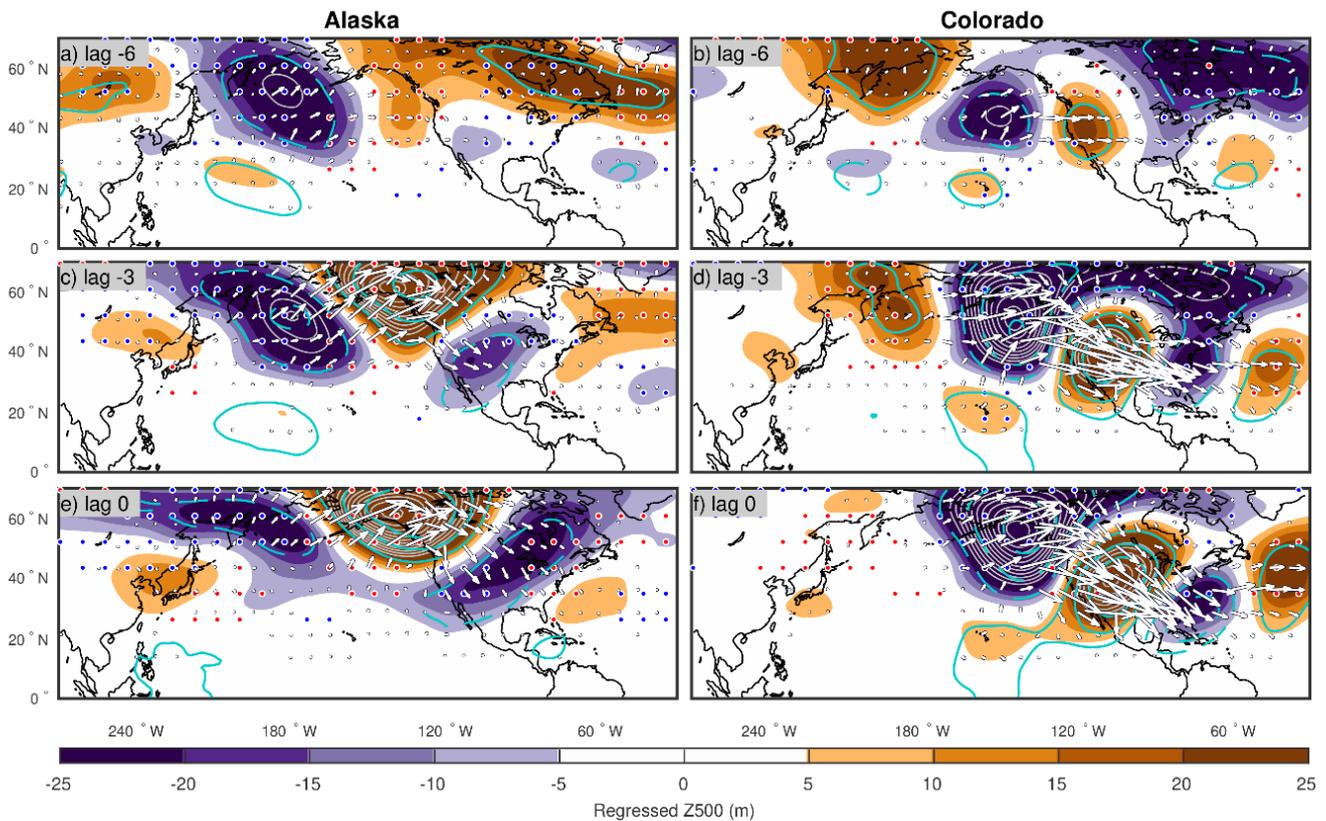
Figure 7: One-point regression maps of Z500 anomalies (colour shading) with respect to reference SAT time series over (left) Alaska (61°N, 150°W) and (right) Colorado (39°N, 105°W). The corresponding correlation is superimposed with cyan contours (increments of 0.2). The regression is performed separately for years when SVD1$_{SST}$ >= 1 and SVD1$_{SST}$ <= −1 (indicated with blue crosses and circles in Fig. 1, respectively) and the average of the two patterns is shown in this figure. The reference SAT time series for the positive and negative phases are normalized independently before carrying out the regression. Differences between the SVD1$_{SST}$ >= 1 and SVD1$_{SST}$ <= −1 patterns that are significant at the 95% level are shown with blue dots for negative differences and red dots for positive differences. The wave-activity flux (Takaya and Nakamura, 2001) evaluated with the regressed Z500 anomalies is shown with white arrows with a distance of 1° corresponding to a flux of 2/3 m² s⁻².
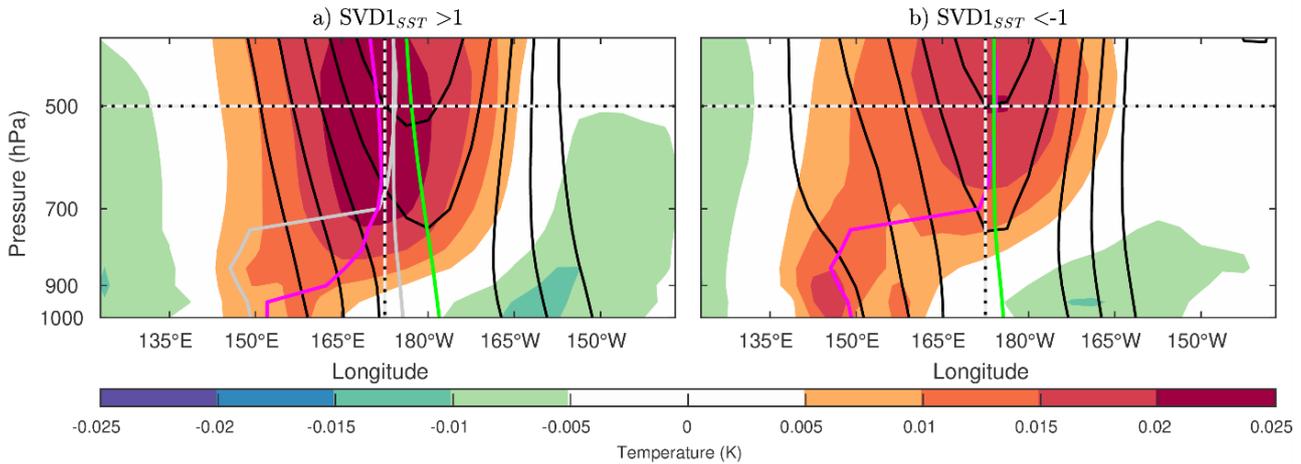
Figure 8: Zonal sections of anomalies of geopotential height anomalies (black contours with intervals of 10 m; solid and dashed lines are used for positive and negative values, respectively) and temperature (shadings) both regressed onto the reference time series of geopotential height at [54°N, 175°W], for winters when a) SVD1$_{SST}$ > 1 and b) SVD1$_{SST}$ < −1. The maxima of geopotential height and temperature at every pressure level are linked with green and magenta lines, respectively. The lines shown in b) are also repeated in grey in a) for comparison.
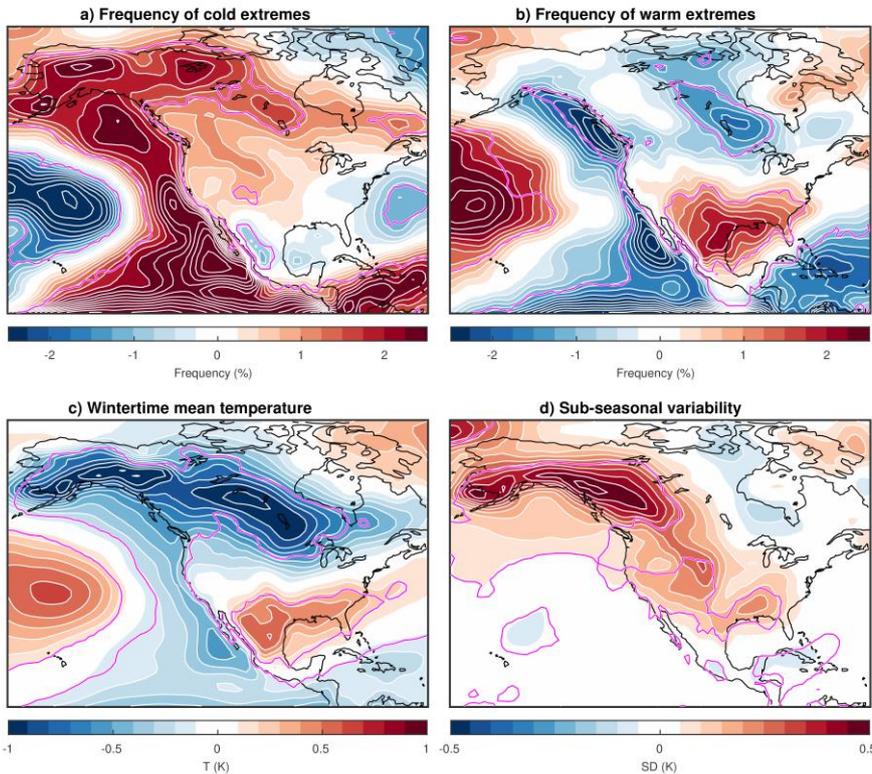
Figure 9: Regression of a) frequency of cold extremes, b) frequency of warm extremes, c) winter-mean SAT, and d) subseasonal SAT variability onto the SVD1$_{SST}$ index. Values that are statistically significant at the 95% confidence level are contoured in magenta.
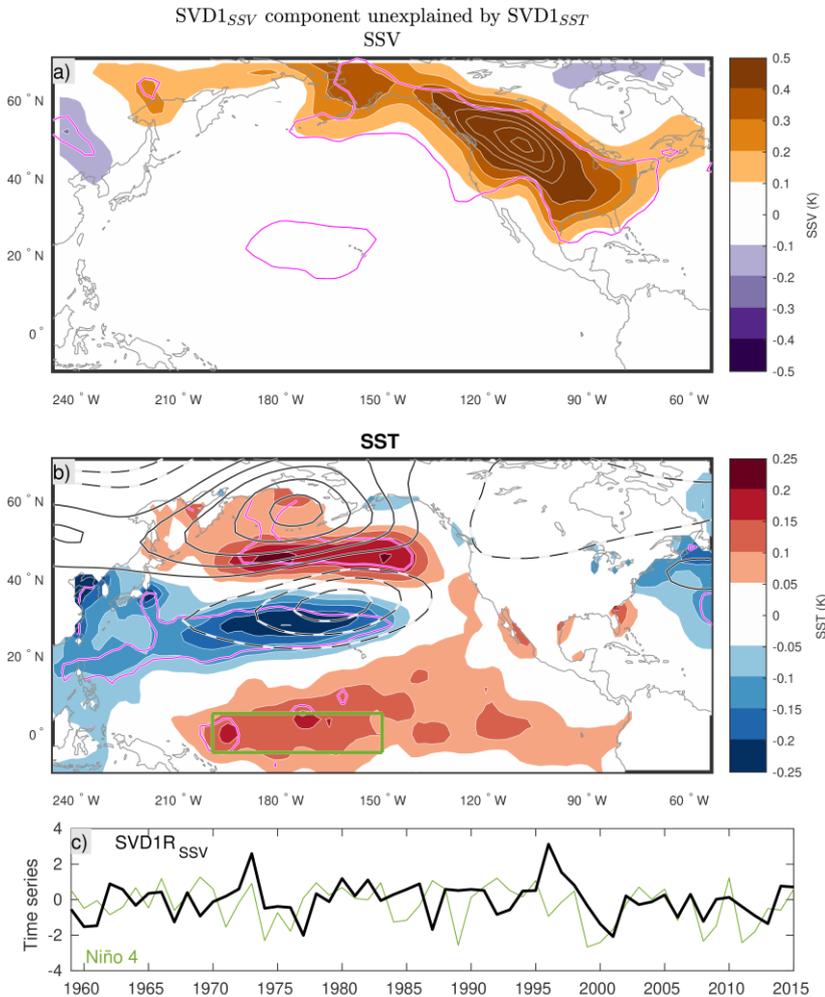
Figure 10: SSV a) and SST b) are regressed on the component of SVD1$_{SSV}$ that is not correlated with SVD1$_{SST}$ (SVD1R$_{SSV}$). Regions that are statistically significant at the 95% level are contoured in magenta. The green contours superimposed on a) indicate the fractional change of SSV relative to the climatology with 5% contour intervals (solid and dashed contours are used for positive and negative values, respectively; the 0 line is omitted). The regression of Z500 (contours, 5 m intervals with solid and dashed black contours for positive and negative anomalies) is also shown in panel b). The SVD1R$_{SSV}$ time series, as well as the four Niño indices considered, are shown in c) and the regions used to compute these indices are illustrated over the SST pattern in b).

510